

# Model-Based Machining Force Control

**Robert G. Landers**

Assistant Research Scientist  
e-mail: landers@umich.edu

**A. Galip Ulsoy**

William Clay Ford Professor of Manufacturing  
e-mail: ulsoy@umich.edu

Department of Mechanical Engineering and  
Applied Mechanics,  
The University of Michigan,  
Ann Arbor, MI 48109-2125

*Regulating machining forces provides significant economic benefits by increasing operation productivity and improving part quality. Machining force regulation is a challenging problem since the force process varies significantly under normal operating conditions. Since fixed-gain controllers cannot guarantee system performance and stability as the force process varies, a substantial research effort has been invested in the development of adaptive force controllers. However, adaptive controllers can be difficult to develop, analyze, implement, and maintain due to their inherent complexity. Consequently, adaptive machining force controllers have found little application in industry. In this paper, a model-based machining force control approach, which incorporates detailed force process models, is introduced. The proposed design has a simple structure and explicitly accounts for the changes in the force process to maintain system performance and stability. Two model-based machining force controllers are implemented in face milling operations. The stability robustness of the closed-loop system with respect to model parameter uncertainties is analyzed, and the analysis is verified via simulation and experimental studies. [S0022-0434(00)02303-0]*

## Introduction

Maintaining machining forces at a constant level increases productivity, prevents tool breakage, regulates tool deflections that lead to geometric workpiece errors, etc. Early work in machining force control (Koren and Masory [1]) demonstrated that fixed-gain controllers could not maintain system performance and stability as the force process changed, thus, sparking an interest in the development of adaptive machining force controllers. Indeed, a majority of the work in machining force control is devoted to the subject of adaptive techniques (e.g., Daneshmend and Pak, [2], Ulsoy and Koren, [3], Elbestawi et al. [4]). Adaptive controllers estimate force process model parameters on-line and adjust the controller gains accordingly, thus, the need for off-line calibration tests are eliminated. While adaptive controllers are able to account for changes in the force process, these systems must be carefully tuned and exhibit complex, and sometimes undesirable, behavior. Problems commonly encountered in adaptive control systems include bursting, parameter drift, poorly scaled parameters, lack of persistent excitation, and sensitivity to unmodeled dynamics (Åström and Wittenmark [5]). The complex behavior makes these systems difficult to develop, analyze, implement, and maintain. Consequently, adaptive machining force controllers have found little application in industry.

Alternative approaches to adaptive force control have also been considered. One approach (Elbestawi and Sagherian [6], Elbestawi et al. [4]) broke the nonlinear force process system into a linear system coupled with a third order static feed equation which approximated the nonlinear feed term. A deadbeat controller was applied to the linear system and the controller output was used to complete the feed equation. Harder [7] linearized the force process about a nominal feed and applied standard control techniques to regulate the machining force. This approach was augmented in Landers and Ulsoy [8] by explicitly accounting for depth-of-cut information. Another approach (Harder [7]) transformed the static force process into the logarithmic domain, effectively creating a linear force system, and a standard linear controller was utilized. Robust (Rober and Shin, [9]), neural network (Tang et al. [10]), and fuzzy logic (Kim et al. [11]) controllers have also been applied to the machining force regulation problem.

This paper introduces model-based machining force control approaches for force processes with static dynamics and with first-order dynamics. A model-based machining force controller is developed and experimentally implemented for a static force process; namely, a face milling process. The stability robustness analysis of static model-based force control systems is verified via simulation and experimental studies. The face milling force process is static due to the intermittent contact between the inserts and the workpiece. To investigate model-based force controllers for first-order force processes, the feed servo system is intentionally detuned such that the closed-loop feed dynamics (i.e., the transfer function from the actual feed to the command feed) are first-order. Therefore, the force process dynamics (i.e., the transfer function from the force to the command feed) for the detuned system are first-order. A model-based machining force controller is developed and experimentally implemented for this "first-order" force process and the stability robustness analysis of first-order model-based force control systems is verified via simulation and experimental studies.

## Static Force Process

**Process Model.** The structure of static cutting force processes, including cutting speed and nonlinear depth-of-cut effects, is (Elbestawi and Sagherian [6])

$$F(t) = Kd^{\beta}V^{\gamma}f^{\alpha}(t) \quad (1)$$

where  $F$  is the machining force,  $K$  is the process gain,  $d$  is the depth-of-cut,  $V$  is the cutting speed,  $f$  is the feed, and  $\alpha$ ,  $\beta$ , and  $\gamma$  are coefficients describing the nonlinear relationships between the machining force and the process inputs (i.e.,  $f$ ,  $d$ , and  $V$ ). The four variables which must be calibrated for each tool-workpiece combination are  $K$ ,  $\alpha$ ,  $\beta$ , and  $\gamma$ . Typically, the feed is adjusted on-line to regulate the machining force and, therefore, the force process gain may be seen as  $\theta = Kd^{\beta}V^{\gamma}$  which is sensitive to the process inputs. Static models are used when regulating a force signal that is sampled once *per spindle revolution* such as a maximum or average force. Such force signals are typically utilized for cutting processes having inherent force fluctuations during the spindle revolution (e.g., general milling applications).

**Controller Design.** The controller design objectives are to track constant reference forces, reject constant disturbances, follow a specified closed-loop transient behavior, and guarantee no

Contributed by the Dynamic Systems and Control Division for publication in the JOURNAL OF DYNAMIC SYSTEMS, MEASUREMENT, AND CONTROL. Manuscript received by the Dynamic Systems and Control Division October 20, 1999. Associate Technical Editor: T. Kurfess.

steady-state error. The feed drive dynamics are assumed to be sufficiently fast, as compared to the force process response, such that they may be ignored. A change of variable is made and the control variable is defined as

$$u_c \equiv f^{\alpha^*} \quad (2)$$

where  $\alpha^*$  is an off-line estimate of  $\alpha$ . Including a zero order hold (ZOH), the static force process model in the discrete time domain used for controller design is

$$F(z) = \theta^* u_c(z) \quad (3)$$

where  $z$  is the discrete-time forward shift operator and  $\theta^* = K^* d^{\beta^*} V^{\gamma^*}$  is an off-line estimate of the force process gain. Therefore, the force process gain estimate is a function of off-line estimates of model parameters (i.e.,  $K^*$ ,  $\beta^*$ , and  $\gamma^*$ ) and on-line measurements of cutting conditions (i.e.,  $d$  and  $V$ ). Now a variety of simple, linear control techniques may be utilized for the controller design. The change of variable made in Eq. (2) allows the designer to directly incorporate the force-feed nonlinearity. Further, the force process gain estimate may be changed on-line as the cutting conditions change (e.g., a new spindle speed reference may be selected to suppress chatter or the depth-of-cut may change due to the workpiece geometry). This allows the force controller to adjust for changing cutting conditions and directly incorporate the nonlinear process effects.

The force controller will require integral action to ensure the tracking and disturbance rejection specifications. Therefore, the force process model in Eq. (3) is augmented with an integral state and the Model Reference Control (MRC) technique is used to design the following control law

$$u_c(z) = \frac{1}{z-1} \frac{1+b_0}{\theta^*} [F_r(z) - F(z)] \quad (4)$$

where the polynomial  $z+b_0=0$  defines the desired closed-loop dynamics. The control variable must be positive to calculate the commanded feed (see Eq. (8)); therefore, the control variable is bounded from below by

$$u_{\min}(k) = f_{\min}^{\alpha^*}(k) > 0 \quad (5)$$

where  $f_{\min}$  is typically selected to be an arbitrarily small, positive number. However,  $f_{\min}$  may be selected from process considerations (e.g., to ensure chip breaking in turning). A maximum feed, typically selected from machining handbooks or some machining process criteria (e.g., tooth chippage) is also set; therefore, the control variable is bounded from above by

$$u_{\max}(k) = f_{\max}^{\alpha^*}(k) \quad (6)$$

The applied control variable is

$$u(k) = \begin{cases} u_{\min}(k) & \text{if } u_c(k) < u_{\min}(k) \\ u_c(k) & \text{if } u_{\min}(k) \leq u_c(k) \leq u_{\max}(k) \\ u_{\max}(k) & \text{if } u_c(k) > u_{\max}(k) \end{cases} \quad (7)$$

The commanded feed at the  $k$ th iteration, found through the inverse of Eq. (2), is

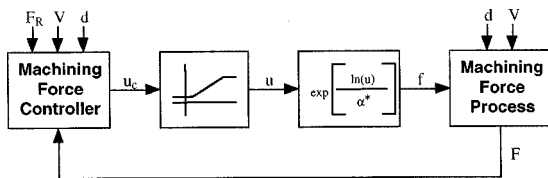


Fig. 1 Block diagram of model-based machining force control system

$$f(k) = \exp\left\{\frac{\ln[u_c(k)]}{\alpha^*}\right\} \quad (8)$$

A block diagram of the complete machining force control system is shown in Fig. 1. An experimental implementation of the model-based force controller for a static force process is shown in a subsequent section.

**Stability Analysis.** The closed-loop dynamics of the controlled static force process is found by converting Eqs. (1), (2), and (4) into difference equations. Combining these difference equations yields

$$f^{\alpha^*}(k) = f^{\alpha^*}(k-1) + \frac{1+b_0}{\theta^*} [F_R - \theta^* f^{\alpha^*}(k-1)] \quad (9)$$

where  $F_R$  is the value of the constant reference machining force. Applying linearization techniques to this system, and ignoring saturation, one equilibrium point is found where  $F = F_R$ . The eigenvalue of the linearized equations about this equilibrium is

$$\lambda = 1 - (1+b_0) \frac{\theta}{\theta^*} \frac{\alpha}{\alpha^*} \frac{f_e^\alpha}{f_e^{\alpha^*}} \quad (10)$$

where  $f_e$  is the feed such that

$$F_R = \theta f_e^\alpha \quad (11)$$

The system will be marginally stable if the eigenvalue is located at 1 or  $-1$ . The eigenvalue will be located at 1 if the desired closed-loop dynamics are designed to be marginally stable (i.e., the parameter  $b_0 = -1$ ) or if the model parameters are selected to be infinite. Since a designer would not select infinite model parameters or design a closed-loop system to be marginally stable, the case where  $\lambda = 1$  is not explored. If the eigenvalue is located at  $-1$ , Eq. (10) may be rewritten as

$$\frac{\theta}{\theta^*} = \frac{2}{(1+b_0)} \frac{\alpha^*}{\alpha} \frac{f_e^{\alpha^*}}{f_e^\alpha} \quad (12)$$

Equation (12) defines the relationship between the model parameters when the closed-loop force control system is marginally stable. As an example, a plot of the stability boundary for a specific set of model parameters is shown in Fig. 2. The simulation results demonstrate the excellent prediction from the linearization analysis; however, there is slight error in the region  $\alpha < \alpha^* < 2\alpha$ .

When the closed-loop force control system operates on the stability borderline (i.e., the model parameters are chosen such that

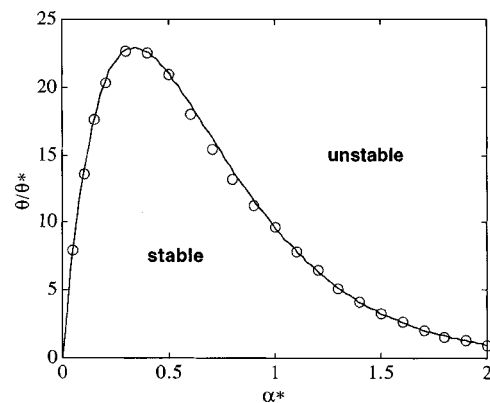
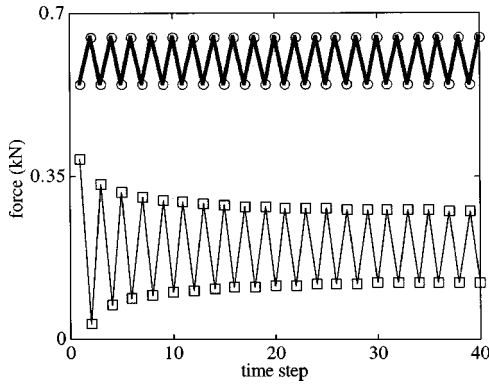


Fig. 2 Stability borderline for machining force control system for static force process. Analysis (line) from Eq. (12) and simulations (circles). Parameters:  $F_R = 0.2$  kN,  $f(0) = 0.2$  mm,  $\alpha = 0.5$ ,  $\theta = 0.8705$ ,  $b_0 = -0.9048$ ,  $f_{\min} = 10^{-10}$  mm, and  $f_{\max} = 1.0$  mm.



**Fig. 3 Marginally stable force responses. In region  $\alpha < \alpha^* < 2\alpha$  (top thick line with circles):  $F_R=0.6$  kN,  $f(0)=0.4$  mm,  $\alpha=0.5$ ,  $\theta=0.8705$ ,  $b_0=-0.9048$ ,  $f_{\min}=10^{-10}$  mm,  $f_{\max}=1.0$  mm,  $\alpha^*=0.5$ , and  $\theta/\theta^*=21.02$ . Outside region  $\alpha < \alpha^* < 2\alpha$  (bottom thin line with squares):  $F_R=0.2$  kN,  $f(0)=0.2$  mm,  $\alpha=0.5$ ,  $\theta=0.8705$ ,  $b_0=-0.9048$ ,  $f_{\min}=10^{-10}$  mm,  $f_{\max}=1.0$  mm,  $\alpha^*=0.3$ , and  $\theta/\theta^*=22.73$ .**

the closed-loop force control system is marginally stable), the dynamic force response in the region  $\alpha < \alpha^* < 2\alpha$  is quite different than the dynamic force response outside of this region (Fig. 3). Outside of this region, the magnitudes of the force error (i.e., the difference between the reference and the actual force) decrease until a constant value is reached. In the region  $\alpha < \alpha^* < 2\alpha$ , the magnitude of the force error is constant, that is

$$F_R - F(k) = F(k+1) - F_R \quad (13)$$

Taking  $k=0$ ,

$$F_R - F(0) = F(1) - F_R \quad (14)$$

The initial force and the force at the first time step, respectively, are

$$F(0) = \theta f^\alpha(0) \quad (15)$$

$$F(1) = \theta f^\alpha(1) = \theta \exp\left\{\frac{\alpha}{\alpha^*} \ln[u(1)]\right\} \quad (16)$$

The initial control variable and the control variable at the first time step, respectively, are

$$u(0) = f^{\alpha^*}(0) \quad (17)$$

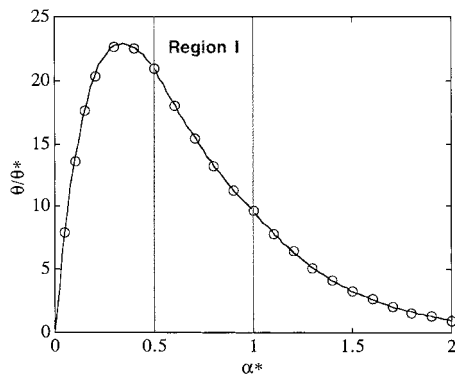


**Fig. 4 Stability borderline for machining force control system for static force process. Analysis (line) from Eq. (12) outside of Region I and from Eq. (19) inside Region I. Simulations (circles). Parameters are given in Fig. 2.**

$$u(1) = u(0) + \frac{1+b_0}{\theta^*} [F_R - \theta f^\alpha(0)] \quad (18)$$

Combining Eq. (11) with Eqs. (14)–(18), the following relationship is derived

$$\theta^* = \frac{[1+b_0][F_R - \theta f^\alpha(0)]}{\exp\left\{\left[\frac{\alpha^*}{\alpha}\right] \ln[2f_e^x - f^\alpha(0)]\right\} - f^{\alpha^*}(0)} \quad (19)$$

Equation (19) determines the stability boundary in the parameter space of the closed-loop force control system in the region  $\alpha < \alpha^* < 2\alpha$  while Eq. (12) determines the stability boundary outside of this region. Figure 4 demonstrates that together, the analyses given by Eqs. (12) and (19) may be combined to perfectly predict the stability boundary in the force model parameter space.

## First-Order Force Process

**Process Model.** The structure of first-order cutting force processes, including cutting speed and nonlinear depth-of-cut effects, is (Daneshmend and Pak [2])

$$F(s) = \frac{Kd^\beta V^\gamma}{\tau s + 1} f^\alpha(s) \quad (20)$$

where  $\tau$  is the force process time constant. Since one spindle revolution is required to develop a full chip load,  $\tau$  is 63 percent of the time required for a spindle revolution (Daneshmend and Pak [2]). In addition to the other model parameters,  $\tau$  must be calibrated for each different tool-workpiece combination. First-order models are typically employed when considering a force signal that is sampled several times per spindle revolution. Such force signals are typically utilized for processes where the tool and workpiece are continually in contact and there are no chip load variations during the spindle revolution (e.g., general turning applications).

**Controller Design.** The control variable is again defined by Eq. (2), a ZOH is included, and the first-order force process model used for controller design is

$$F(s) = \theta^* \frac{1+a^*}{z+a^*} u_c(z) \quad (21)$$

where  $a^*$  is an off-line estimate of the discrete-time pole  $a$  which depends upon the process time constant and the sample period. Again, an integral state is added to the plant to ensure tracking and disturbance rejection specifications and the MRC technique is used to design the control law

$$\begin{aligned} [z-1]u_c(z) &= \frac{1+b_1+b_0}{\theta^*(1+a^*)} zF_r(z) - \frac{(b_1-a^*+1)}{\theta^*(1+a^*)} zF(z) \\ &\quad - \frac{(b_0+a^*)}{\theta^*(1+a^*)} F(z) \end{aligned} \quad (22)$$

where the discrete-time polynomial  $z^2+b_1z+b_0=0$  defines the desired closed-loop dynamics. The minimum control variable, maximum control variable, applied control variable, and commanded feed are again given by Eqs. (5), (6), (7), and (8), respectively, and the force control system is again represented schematically by Fig. 1. An experimental implementation of the model-based force controller for a first-order force process is shown in a subsequent section.

**Stability Analysis.** The closed-loop dynamics of the controlled first-order force process may be found by converting Eqs. (2), (20), and (22) into difference equations. Again, there is one equilibrium point where  $F=F_R=\theta f_e^\alpha$ . Linearization about this point yields the following relationship for the system eigenvalues

$$\lambda^2 + \left[ a - 1 + \eta \frac{\theta}{\theta^*} (b_1 - a^* + 1) \right] \lambda + \left[ -a + \eta \frac{\theta}{\theta^*} (b_0 + a^*) \right] = 0 \quad (23)$$

where

$$\eta = \frac{(1+a)}{(1+a^*)} \frac{\alpha f_e^\alpha}{\alpha^* f_e^{\alpha^*}} \quad (24)$$

There are three distinct conditions for marginal stability.

*Condition 1: closed-loop poles at  $-1$  and  $q$  where  $-1 \leq q \leq 1$*   
For this condition

$$q = \frac{a(b_1 + b_0 + 1) - 2(b_0 + a^*)}{b_1 - b_0 + 1 - 2a^*} \quad (25)$$

and the stability boundary is given by

$$\frac{\theta}{\theta^*} = \frac{1}{\eta} \frac{2(1-a)}{b_1 - b_0 + 1 - 2a^*} \quad (26)$$

*Condition 2: closed-loop poles at  $q_1 \pm q_2 \sqrt{-1}$  where  $q_1^2 + q_2^2 = 1$*

For this condition

$$q_1 = \frac{a-1}{2} + \frac{1+a}{2(b_0 + a^*)} [b_1 - a^* + 1] \quad (27)$$

and the stability boundary is given by

$$\frac{\theta}{\theta^*} = \frac{1}{\eta} \frac{1+a}{b_0 + a^*} \quad (28)$$

*Condition 3: closed-loop poles at  $1$  and  $q$  where  $-1 \leq q \leq 1$*   
For this condition, the stability boundary is given by

$$\frac{\theta}{\theta^*} = 0 \quad (29)$$

This condition is only encountered when the model parameters are selected to be infinite.

From Eqs. (25) and (27), respectively, it can be seen that as  $a^* \rightarrow -\infty$ ,  $q \rightarrow 1$  and as  $a^* \rightarrow \infty$ ,  $q_1 \rightarrow -1$ . The parameter  $A^*$  is defined as

$$A^* \equiv \frac{(a+1)(b_1+1) + b_0(a-3)}{4} \quad (30)$$

When  $a^* = A^*$ ,  $q = -1$  and  $q_1 = 1$ . The derivatives of  $q$  and  $q_1$  with respect to  $a^*$ , respectively, are

$$\frac{\partial q}{\partial a^*} = \frac{(a-1)(b_1 + b_0 + 1)}{(b_1 - b_0 + 1 - 2a^*)^2} \quad (31)$$

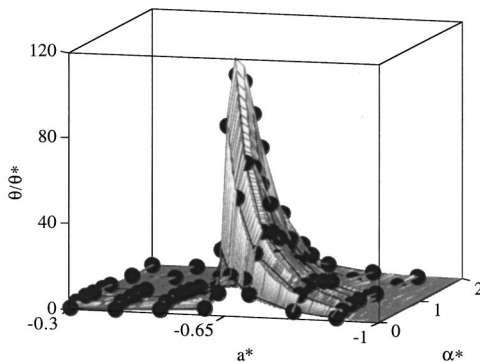


**Fig. 5** Stability borderline generated by linearization analysis (surface) and verified via simulations (spheres). Simulation parameters:  $F_R = 0.4$  kN,  $f_0 = 0.1$  mm,  $\alpha = 0.7$ ,  $\theta = 2.0$ ,  $a = -0.8206$ ,  $b_1 = -1.562$ , and  $b_0 = 0.6413$ . The parameter  $A^* = -0.6377$ .

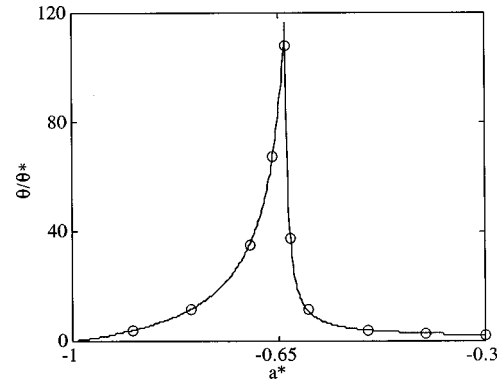


**Fig. 6** Stability borderline (linearization analysis-line, simulations-circles) for  $\alpha^* = 0.6$  and simulation parameters given in Fig. 5. The parameter  $A^* = -0.6377$ .

$$\frac{\partial q_1}{\partial a^*} = \frac{-(1+a)(b_1 + b_0 + 1)}{2(b_0 + a^*)^2} \quad (32)$$

Since the force process is overdamped and stable,  $-1 < a < 0$  and, from Jury's test,  $b_1 + b_0 + 1 > 0$ . Therefore, the derivatives in Eqs. (31) and (32) are always negative,  $-1 \leq q \leq 1$  for  $-\infty \leq a^* \leq A^*$ , and  $-1 \leq q_1 \leq 1$  for  $A^* \leq a^* \leq \infty$ . Thus, the stability boundary is described by Eq. (26) for  $-\infty \leq a^* \leq A^*$  and by Eq. (28) for  $A^* \leq a^* \leq \infty$ .

The stability analysis is verified via the simulation study shown in Fig. 5. For a given value of  $a^*$ , the stability borderline is similar to that shown in Fig. 2. Therefore, the control system has excellent stability robustness with respect to variation in  $\alpha$ . Figure 6 shows a slice of the stability surface for a constant value of  $\alpha^*$ . When  $a^* = A^*$ , the robustness with respect to variations in  $\theta^*$  is large; however, as the ratio of  $\theta/\theta^*$  increases, the robustness with respect to variations in  $a^*$  decreases. Note that selecting  $a^* = a$  does not necessarily provide the optimal stability robustness with respect to model parameter variations. Again, the analytical results provide a systematic means of selecting controller parameters.

### Additional Force Process Effects

The force process models presented above do not incorporate such effects as tool angles, chip load variations due to runout, tooth entry/exit, etc., tool wear, cutting temperature, and undesirable conditions such as chatter and chip entanglement. To include these effects, the force process models would need to be expanded. Mechanistic models capture the effect of tool angles; however, these angles are typically fixed throughout the operation and do not explicitly appear in the force process model. Chip load variations, also captured by mechanistic models, are unavoidable in certain machining operations (e.g., general milling applications). Therefore, an average or maximum force per spindle revolution is typically utilized, leading to a static force process. Tool wear and cutting temperature also affect machining forces; however, these models at present are not general and, thus, are usually not included in the force process design model. Typically, the effect of tool wear and cutting temperature on the force process model must be determined and the controller must be designed, using the stability analysis presented above, to be robust to these effects. As was seen above, stability robustness with respect to gain uncertainty of an order of magnitude or more may easily be obtained with the controllers developed in this paper. This stability robustness is more than sufficient for the gain variations due to tool wear reported in the literature (e.g., Park and Ulsoy [12]). Lastly, undesirable conditions such as chatter and chip entangle-

ment are not included in the force process model since these conditions do not occur if the operation is properly planned or are eliminated upon detection.

It should be noted that some models utilized for machining force controller design are greater than first-order (e.g., Furness et al. [13]). These models incorporate the feed drive dynamics. If the feed drive dynamics are sufficiently fast as compared to the process dynamics, the feed drive dynamics may be ignored, making for a less complex controller design. Since the desired process dynamics are typically much slower than the dynamics of the servo system, this design separation is natural. If the designer requires a relatively quick process response relative to the servo response, a model of the feed drive dynamics needs to be combined with the force process model.

### Experimental Studies: Static Force Process

Experimental studies are now conducted for a face milling operation to verify the stability analysis conducted above of model-based force control systems for static force processes and to explore the effect of controller parameters on the closed-loop system stability. A schematic of the experimental system is shown in Fig. 7. The objective of the force control system is to maintain maximum productivity given a spindle power constraint. With a constant spindle speed of 1500 rpm, a maximum spindle power of 1.5 hp, and a tool radius of 25 mm, the maximum cutting force is 0.285 kN. The force signal that will be regulated is

$$F_y = \max\{|f_y^1|, \dots, |f_y^N|\} \quad (33)$$

where  $f_y$  is the instantaneous force in the  $y$  direction and  $N$  is the number of samples during two spindle rotations. This force signal bounds the cutting force (Landers [14]). A sample period of 0.5 ms is used to collect the individual force samples (i.e.,  $f_y^1, \dots, f_y^N$ ), thus,  $N=160$  and the force controller sample period is 0.08 s.

A series of tests were conducted for a range of feeds and depths-of-cut (Landers [14]) and the following force process model was developed

$$F_y = 0.76d^{0.65}f^{0.63} \quad (34)$$

An experiment with a step change in the command feed (Fig. 8) illustrates that the open-loop force process can be modeled as a static process. This model does not depend upon cutting speed and tool angles since these values were constant for all experiments, or chatter and chip interference as these conditions were not encountered. The workpiece was prepared such that the tooth entry and exit angles remained constant throughout the entire operation even for experiments having a step change in the depth-of-cut (see

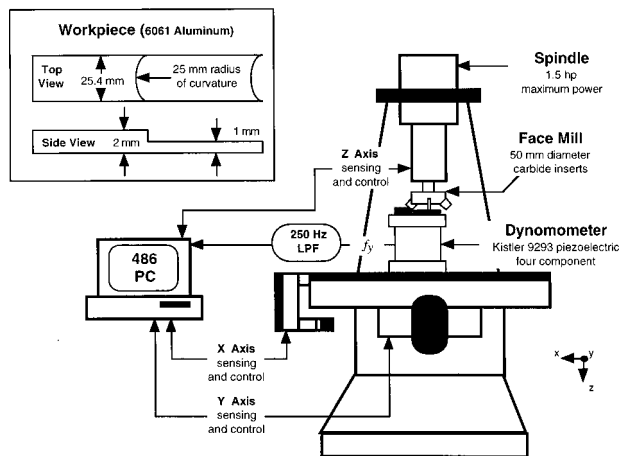


Fig. 7 Schematic of experimental machining system and workpiece

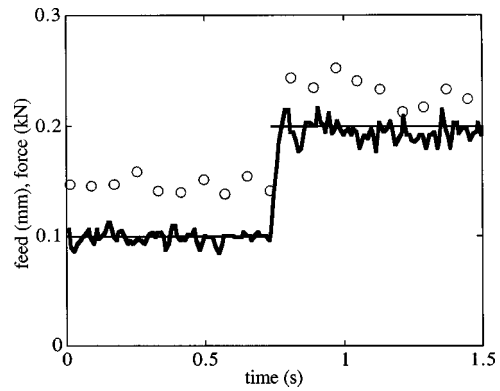


Fig. 8 Force (circles) and feed (thick line) responses to step change in commanded feed (thin line) for static system. Force sample period is 0.08 s and feed sample period is 0.01 s.

Fig. 7). Runout does not affect the force process since a maximum force per two spindle revolutions is the regulated signal. Also, inserts were changed frequently enough such that tool wear did not have a noticeable effect on the force process. A model-based force controller was developed and implemented experimentally (Fig. 9) for a workpiece prepared with a step change in the depth-of-cut.

Simulations and experiments were also conducted to verify the stability analysis and explore the effects of controller parameters on closed-loop system stability. The data points were determined by adjusting the estimated force process gain ( $\theta^*$ ) incrementally until instability was encountered as indicated by sustained saturation in the control and output signals. The stability border in the  $\alpha^* - \theta/\theta^*$  plane is plotted for desired closed-loop time constants of  $\tau_c=0.8$  and 1.6 s (i.e.,  $b_0=-0.9048$  and  $b_0=-0.9572$ , respectively) in Fig. 10. The simulations and experiments are in excellent agreement with the analysis. Since typical values for  $\alpha$  range from 0.5 to 0.8, the model-based controller has sufficient robustness to uncertainty in  $\alpha$ . For most machining applications, variations of  $\theta$  will be well within an order of magnitude if changes in process parameters are taken into account; therefore, the model-based controller has sufficient robustness with respect to uncertainty in  $\theta$ , too. The studies have also illustrated the naturally intuitive result that greater stability margins are obtained when closed-loop performance is decreased. Thus, the analysis tool may be used by the designer to make this tradeoff in a systematic manner.

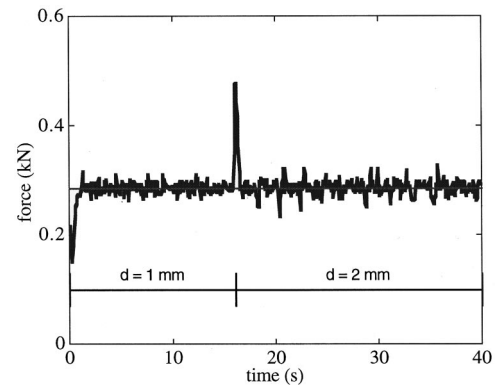
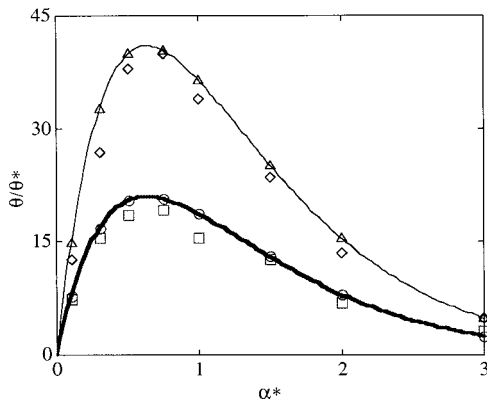


Fig. 9 Force response (thick line) for static model-based force controller. Parameters:  $F_R=0.285$  kN (thin line),  $\alpha^*=0.63$ ,  $\theta^*=1.0$ ,  $f(0)=0.1$  mm,  $f_{\min}=10^{-4}$  mm,  $f_{\max}=0.4$  mm, and  $\tau_c=0.4$  s ( $b_0=-8187$ ).



**Fig. 10** Stability borderline of model-based machining force control system for a static force process. Analysis (thick line), simulations (circles), and experiments (squares) for  $\tau_c=0.8$  s ( $b_0=-0.9048$ ). Analysis (thin line), simulations (triangles), and experiments (diamonds) for  $\tau_c=1.6$  s ( $b_0=-0.9512$ ). Experimental parameters:  $F_R=0.285$  kN,  $f(0)=0.2$  mm,  $\alpha=0.63$ ,  $\theta=0.76$ ,  $f_{\min}=10^{-4}$  mm, and  $f_{\max}=0.4$  mm.

### Experimental Studies: First-Order Force Process

The force process for the face milling operation is a static process (i.e., the transfer function of the force to the command feed is static) since the feed dynamics are relatively fast. To evaluate the performance and stability robustness of model-based machining force controllers developed for first-order force processes, the feed servo system is intentionally detuned. The parameters for the  $x$ -axis (i.e., the feed axis) servo control system are adjusted such that the transfer function from the actual feed to the command feed is a first-order system. Thus, the force process dynamics (i.e., the transfer function from the force to the command feed) of the detuned system are also first-order. An experiment with a step change in the command feed for the first-order system (Fig. 11) illustrates that the open-loop force process may be modeled as a first-order system with a time constant of 0.5 s. The first-order force process model is

$$F_Y = \frac{0.11}{z - 0.85} d^{0.65} f^{0.63} \quad (35)$$

This system is utilized below to evaluate model-based machining force controllers for first-order force processes. A model-based force controller was developed and implemented experimentally (Fig. 12) for a workpiece prepared with a step change in the depth-of-cut.

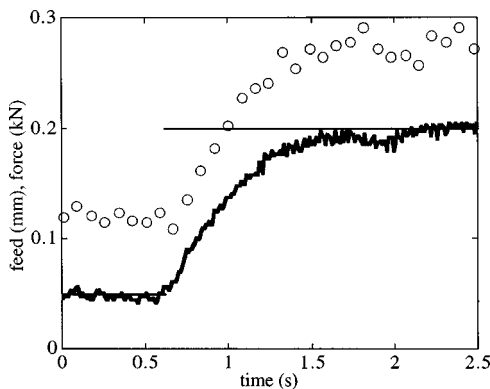


**Fig. 11** Force (circles) and feed (thick line) responses to step change in commanded feed (thin line) for first-order system. Force sample period is 0.08 s and feed sample period is 0.01 s.

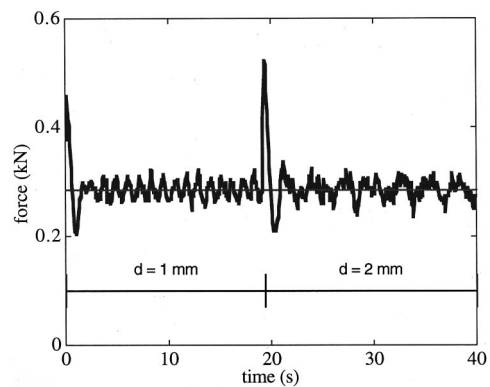


**Fig. 12** Force response (thick line) for first-order model-based force controller. Parameters:  $F_R=0.285$  kN (thin line),  $a^*=-0.85$ ,  $\alpha^*=0.63$ ,  $\theta^*=1.0$ ,  $f_0=0.4$  mm,  $f_{\min}=10^{-4}$  mm,  $f_{\max}=0.6$  mm, and  $\omega_c=\pi$  rad/s and  $\zeta_c=0.7071$  ( $b_1=-1.6480$  and  $b_0=0.7009$ ).

Simulation and experimental studies were conducted to verify the stability analysis and explore the effects of controller parameters on system stability. The stability border in the  $a^*-\theta/\theta^*$  plane is plotted for closed-loop natural frequencies of  $\omega_c=\pi$ ,  $2\pi$ , and  $4\pi$  rad/s in Fig. 13. The simulations are in excellent agreement with the analysis; however, while the experiments agreed with the robustness analysis in the  $a^*$  direction, the analysis over-predicted the stability margin in the  $\theta/\theta^*$  direction near  $a^*=A^*$ . This disagreement is due to the sensitivity of the controller to feedback noise when the gains are large (i.e., around  $a^*=A^*$ ). The high gains cause saturation in the controller even when a small amount (e.g., less than 5 percent) of noise is present in the feedback signal. However, the results demonstrate sufficient stability margins may be obtained with the model-based force controller with respect to uncertainties in  $a$ ,  $\alpha$ , and  $\theta$ . The studies also illustrate that the controller parameters greatly influence the shape of the stability borderline. As a slower response is desired, the stability margin in the  $\theta/\theta^*$  direction increases while the stability margin in the  $a^*$  direction *decreases*. Another interesting result is that for certain ranges of controller parameters, the stability robustness at  $a^*=a$  in the  $\theta/\theta^*$  direction is small, a result that is

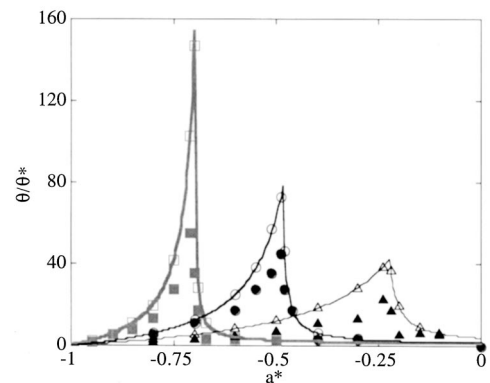


**Fig. 13** Stability borderline of model-based machining force control system for a first-order force process. Analysis (thick line), simulations (empty squares), and experiments (solid squares) for  $\omega_c=\pi$  rad/s. Analysis (medium line), simulations (empty circles), and experiments (solid circles) for  $\omega_c=2\pi$  rad/s. Analysis (thin line), simulations (empty triangles), and experiments (solid triangles) for  $\omega_c=4\pi$  rad/s. Experimental parameters:  $F_R=0.285$  kN,  $f_0=0.2$  mm,  $\alpha=0.63$ ,  $a=-0.85$ ,  $\theta=0.76$ ,  $f_{\min}=10^{-4}$  mm,  $f_{\max}=0.6$  mm, and  $\zeta_c=0.7071$ .

quite counterintuitive. As an example, consider the system in Fig. 13. While the parameter  $a = -0.85$ , one would not want to select  $a^* = a$  for  $\omega_c = 2\pi$  or  $4\pi$  rad/s. Again, the analysis provides the designer with a means of selecting controller parameters to maintain the required stability robustness to parameter variations.

## Summary and Conclusions

A model-based machining force control approach for static and first-order force processes has been presented. This approach incorporates a detailed model of the machining force process and uses a transformation to employ linear control techniques even though the force process design model is nonlinear. A stability robustness analysis of the closed-loop system with respect to parameter uncertainty was performed and the results demonstrate that the model-based technique is robust to typical force process parameter variations.

The most common force control approach found in the literature is the adaptive approach. This approach requires no knowledge of the force process parameters since the parameters are estimated on-line. Therefore, the adaptive approach is well suited to environments where workpiece and tool materials change often and modeling each combination is economically infeasible (e.g., one-off production and job shops). The model-based approach presented here requires the development of a force process model. Thus, this approach is well suited to situations where the models are available or to production environments with large batch sizes where model development is economically feasible. The cost of this model development may be justified in many situations as force process models may also be utilized in the planning, analysis, monitoring, and control of other aspects of the machining operation (e.g., chatter analysis and process planning) and the model greatly aids in the controller development and analysis. Further, the simplicity of the model-based approach makes it attractive for industrial use.

The model-based machining force control approach presented in this paper incorporates a force process model and, thus, provides excellent performance over a wide range of variation in the process inputs. As machining force modeling becomes more sophisticated and systematically accounts for effects such as tool wear, these effects can be directly incorporated into the model-based force control approach. Until then, the stability analysis presented in this paper provides a systematic means of selecting controller parameters and model parameter estimates to achieve the necessary stability robustness.

## Acknowledgments

The authors gratefully acknowledge the financial support of the National Science Foundation (Grant DDM-9313222) and the University of Michigan's Engineering Research Center for Reconfigurable Machining Systems (NSF Grant EEC95-92125).

## References

- [1] Koren, Y., and Masory, O., 1981, "Adaptive Control with Process Estimation," *CIRP Ann.*, **30**, No.1, pp. 373-376.
- [2] Daneshmend, L. K., and Pak, H. A., 1986, "Model Reference Adaptive Control of Feed Force in Turning," *ASME J. Dyn. Syst., Meas., Control*, **108**, No. 3, pp. 215-222.
- [3] Ulsoy, A. G., and Koren, Y., 1989, "Applications of Adaptive Control to Machine Tool Process Control," *IEEE Control Syst. Mag.*, **9**, No. 4, pp. 33-37.
- [4] Elbestawi, M. A., Mohamed, Y., and Liu, L., 1990, "Application of Some Parameter Adaptive Control Algorithms in Machining," *ASME J. Dyn. Syst., Meas., Control*, **112**, No. 4, pp. 611-617.
- [5] Aström, K. J., and Wittenmark, B., 1995, *Adaptive Control*, 2nd ed., Addison-Wesley, New York.
- [6] Elbestawi, M. A., and Sagherian, R., 1987, "Parameter Adaptive Control in Peripheral Milling," *Int. J. Mach. Tools Manuf.*, **27**, No. 3, pp. 399-414.
- [7] Harder, L., 1995, "Cutting Force Control in Turning-Solutions and Possibilities," Ph.D. dissertation, Department of Materials Processing, Royal Institute of Technology, Stockholm.
- [8] Landers, R. G., and Ulsoy, A. G., 1996, "Machining Force Control Including Static, Nonlinear Effects," *Japan-USA Symposium on Flexible Automation*, Boston MA, July 7-10, pp. 983-990.
- [9] Rober, S. J., Shin, Y. C., and Nwokah, O. D. I., 1997, "A Digital Robust Controller for Cutting Force Control in the End Milling Process," *ASME J. Dyn. Syst., Meas., Control*, **119**, No. 2, pp. 146-152.
- [10] Tang, Y. S., Hwang, S. T., and Wang, Y. S., 1994, "Neural Network Controller for Constant Turning Force," *Int. J. Mach. Tools Manuf.*, **34**, No. 4, pp. 453-460.
- [11] Kim, M. K., Cho, M. W., and Kim, K., 1994, "Applications of the Fuzzy Control Strategy to Adaptive Force Control of Non-Minimum Phase and Milling Operations," *Int. J. Mach. Tools Manuf.*, **34**, No. 5, pp. 677-696.
- [12] Park, J.-J., and Ulsoy, A. G., 1992, "On-Line Tool Wear Estimation Using Force Measurement and a Nonlinear Observer," *ASME J. Dyn. Syst., Meas., Control*, **114**, No. 4, pp. 666-672.
- [13] Furness, R. J., Tsao, T.-C., Rankin, J. S., Muth, M. J., and Manes, K., 1999, "Torque Control for a Form Tool Drilling Operation," *IEEE Trans. Control Syst. Technol.*, **7**, No. 1, pp. 22-30.
- [14] Landers, R. G., 1997, "Supervisory Machining Control: A Design Approach Plus Force Control and Chatter Analysis Components," Ph.D. dissertation, Department of Mechanical Engineering and Applied Mechanics, the University of Michigan, Ann Arbor, MI.